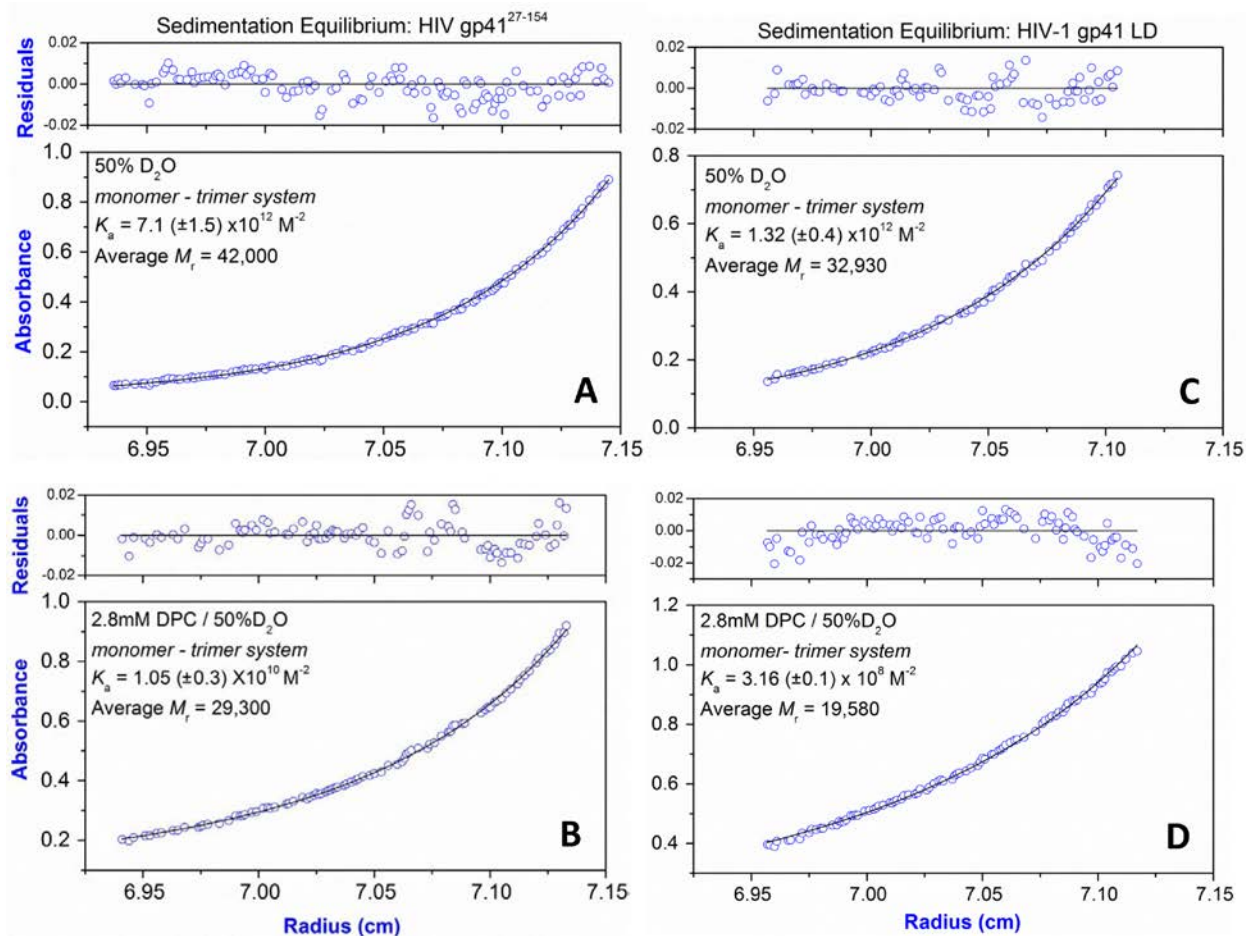


## Supplemental Data

### Supplemental Figures



**Figure S1.**

**Analytical Ultracentrifugation** (relates to Results section “Monomer-Trimer Equilibrium” and Figure 4).

Sedimentation equilibrium data of the HIV-1 ectodomain gp41<sup>27-154</sup> in the absence of detergent (A) and in the presence of dodecyl phosphocholine (DPC, B) are shown. For comparison a loop deletion mutant (gp41 LD) of the gp41 ectodomain has been studied where the immunodominant loop region has been replaced by a six residue flexible linker. The monomer-trimer equilibrium has been analyzed in the absence (C) and presence of DPC (D). Panels are absorbance (bottom panel) and residuals (upper panel). Opened circles show 280nm absorbance gradients in the centrifuge cell. The solid line indicates the calculated fit for the monomer-trimer association. Residuals show the difference in the fitted and experimental values as a function of radial position. The average molecular weights were fitted using an ideal single species model (not shown) which made no assumptions about associative behavior.

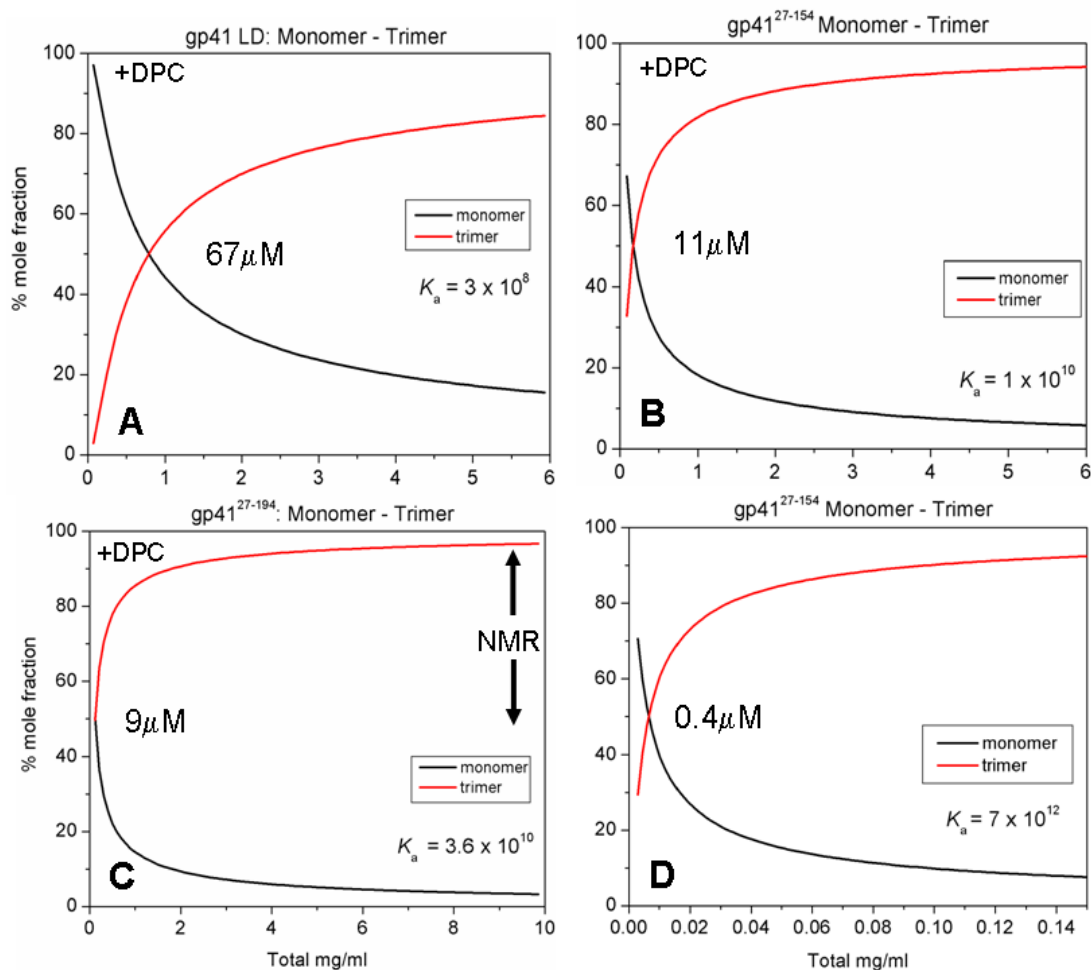


**Figure S2.**

**Profiles of mole fraction of monomer and trimer species plotted as function of total protein concentration** (related to the Results “Monomer-Trimer Equilibrium” and Figure 4).

The concentration profiles were constructed using the  $K_a$  values indicated and which were derived from sedimentation equilibrium measurements (Figure 4 and Figure S1). Panels A-C, refer to  $K_a$  values derived from centrifugation performed in the presence of DPC and Panel D, in the absence of DPC. Panel A, gp41 LD (where IL in gp41<sup>27-154</sup> was replaced with 6 residue flexible linker): 11.83 kDa (1mg/ml = 84.5μM); Panel B, gp41<sup>27-154</sup>: 14.90 kDa (1mg/ml = 67μM); Panel C, gp41<sup>27-194</sup>: 19.65 kDa (1mg/ml = 50.9μM); Panel D, same as B. In all panels, the concentration (μM) corresponding to ~ 50% monomer ~ 50% trimer is indicated.

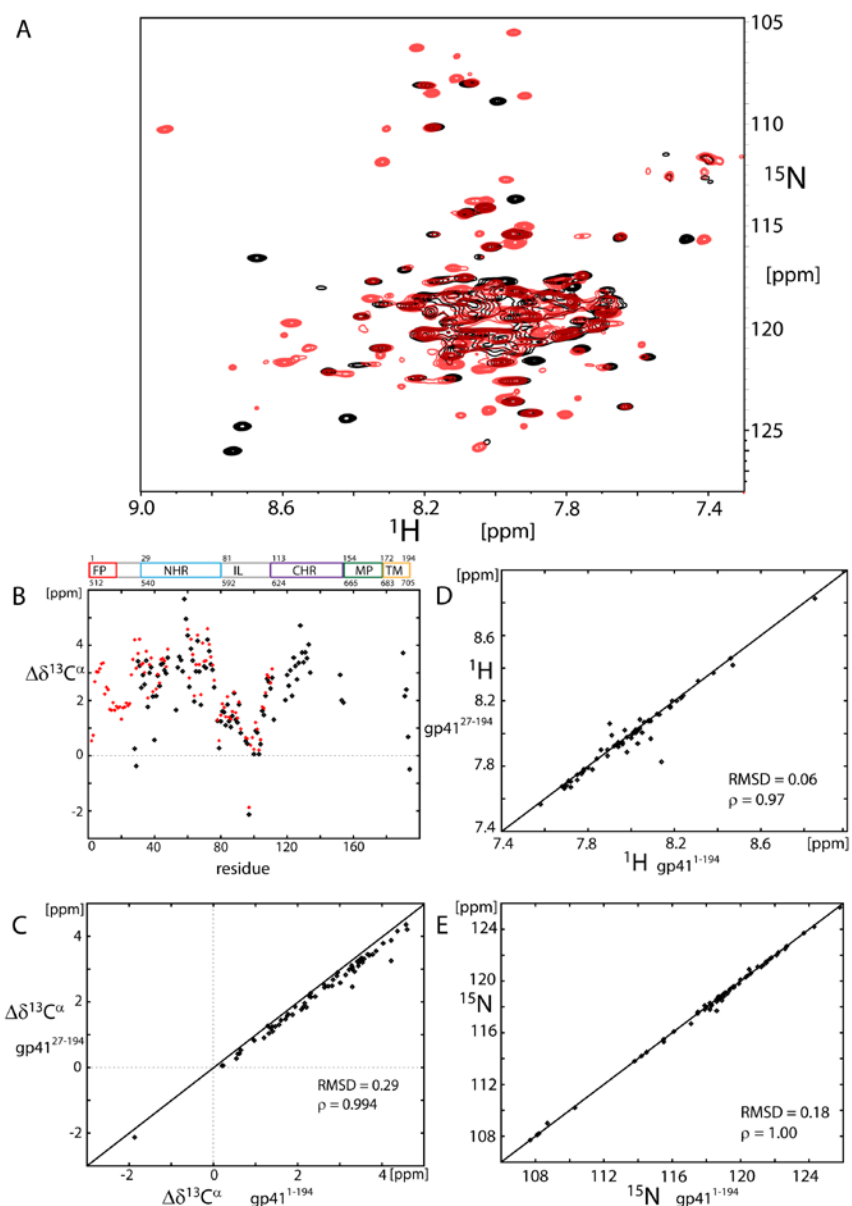


**Figure S3.**

**Comparison of chemical shifts for gp41<sup>27-194</sup> and gp41<sup>1-194</sup> (comprising FP and FPPR),** related to the Results section “Comparison of gp41<sup>27-194</sup> and gp41<sup>1-194</sup> including the fusion peptide” and Figure 1.

Comparison of chemical shifts: **(A)** Overlay of 800 MHz <sup>15</sup>N-<sup>1</sup>H TROSY-HSQC spectra of <sup>2</sup>H<sup>15</sup>N<sup>13</sup>C enriched gp41<sup>27-194</sup> (black) and gp41<sup>1-194</sup> (red) (Lakomek et al., 2013). **(B)** Δδ<sup>13</sup>C<sup>α</sup> secondary chemical shifts of gp41<sup>1-194</sup> (red) are compared to those of gp41<sup>27-194</sup> (black). **(C)** Correlation graph of Δδ<sup>13</sup>C<sup>α</sup> values for residues 30-110 of gp41<sup>1-194</sup>, comparing values measured for gp41<sup>27-194</sup>. Δδ<sup>13</sup>C<sup>α</sup> correlate very well between gp41<sup>27-194</sup> and gp41<sup>1-194</sup> but are slightly reduced in magnitude for gp41<sup>27-194</sup>. **(D)** Correlation graph of <sup>1</sup>H chemical shifts of residues 32-110 of gp41<sup>27-194</sup>, comparing values measured for gp41<sup>1-194</sup>. **(E)** Correlation graph of <sup>15</sup>N chemical shifts of residues 31-110 of gp41<sup>27-194</sup>, comparing values measured for gp41<sup>1-194</sup>.

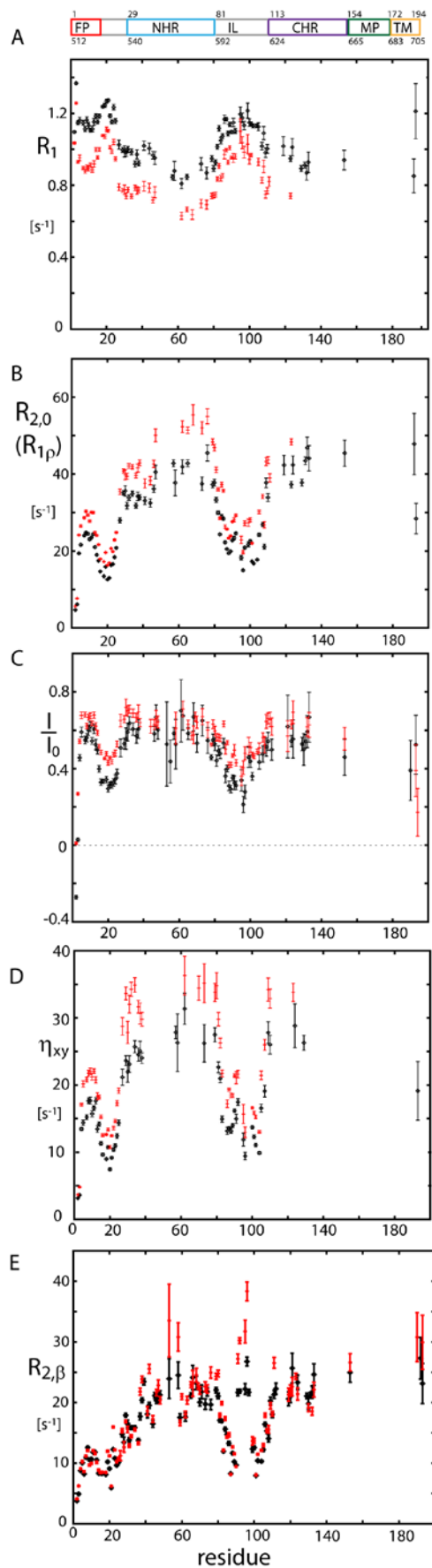


**Figure S4**

**Extended analysis of gp41<sup>1-194</sup> relaxation data** (relates to Results section “Comparison of gp41<sup>27-194</sup> and gp41<sup>1-194</sup> including the fusion peptide” and Figure 2).

<sup>15</sup>N relaxation data recorded for gp41<sup>1-194</sup> in DPC micelles (Lakomek et al., 2013); additional resonances in the 2D spectra could be assigned based on comparison to gp41<sup>27-194</sup>: (A) <sup>15</sup>N R<sub>1</sub> relaxation data at 600 MHz (black) and 800 MHz (red) are highly consistent for both fields. (B) R<sub>2,0</sub> relaxation data (derived from R<sub>1ρ</sub> with a 2 kHz RF field; R<sub>1</sub> contribution corrected) at 600 MHz (black) and 800 MHz (red). (C) <sup>15</sup>N-<sup>1</sup>H NOE values. (D) Transverse CSA-dipolar cross-correlated relaxation rates η<sub>xy</sub>. (E) <sup>15</sup>N R<sub>2,β</sub>.

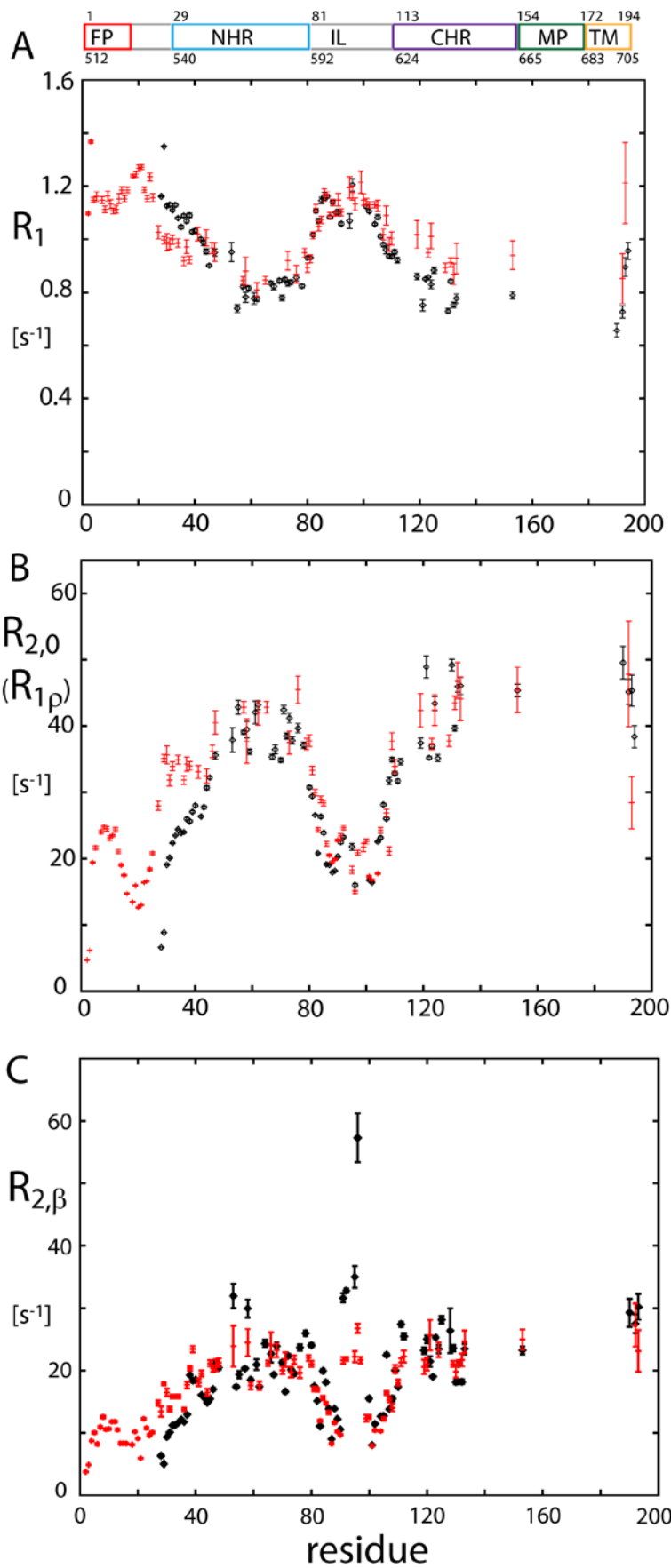


**Figure S5**

Comparison of  $^{15}\text{N}$  relaxation data recorded at 600 MHz for gp41<sup>1-194</sup> in DPC micelles (red) (Lakomek et al., 2013) compared to rates measured for gp41<sup>27-194</sup> (black), related to Figure 2.

Panel (A) shows  $^{15}\text{N}$   $R_1$ , (B)  $^{15}\text{N}$   $R_{2,0}$  relaxation data (derived from  $R_{1\rho}$  with a 2 kHz RF field;  $R_1$  contribution corrected), (C)  $^{15}\text{N}$   $R_{2,\beta}$ . Relaxation data for gp41<sup>1-194</sup> are very similar compared to gp41<sup>27-194</sup>, major differences occur only for residues V28-R45 which are N-terminal in gp41<sup>27-194</sup>, we, thus, consider them as a result of truncation.

## $\Delta\delta^{13}\text{C}^{\alpha}$ secondary chemical shift

**Table S1.**  $\Delta\delta^{13}\text{C}^{\alpha}$  secondary chemical shift for gp41<sup>27-194</sup> (related to the Results section “Secondary structure analysis” and Figure 1).

AA	$\Delta\delta^{13}\text{C}^{\alpha}$	AA	$\Delta\delta^{13}\text{C}^{\alpha}$
	[ppm]		[ppm]
V28	0.25	G86	1.04
Q29	-0.38	A87	1.44
A30	3.42	S88	2.27
R31	3.25	G89	1.31
Q32	2.46	K90	1.20
L33	2.93	L91	1.86
L34	2.58	I92	0.82
S35	3.45	T95	0.53
G36	1.77	A96	0.43
I37	3.00	V97	-2.13
V38	3.20	N100	0.06
Q39	2.15	A101	0.91
Q40	0.57	S102	0.84
Q41	2.16	W103	0.06
N42	2.90	S104	0.42
N43	2.53	N105	1.63
L44	3.31	K106	1.47
L45	3.34	S107	2.17
R46	3.10	L108	2.79
A47	2.98	E109	2.67
I48	3.55	Q110	2.44
H53	1.66	I111	2.83
L54	3.20	W112	1.30
L55	3.58	E119	2.02
Q56	3.46	W120	2.92
L57	3.06	D121	2.54
T58	5.67	R122	3.09
V59	4.95	E123	2.17
W60	4.36	I124	3.55
G61	2.49	N125	3.25
I62	3.87	N126	2.76
K63	3.45	Y127	3.36
Q64	1.96	T128	4.71
L65	3.06	S129	3.74
Q66	4.16	L130	3.38

A67	3.05	I131	3.74
R68	1.84	H132	3.53
L70	3.23	S133	4.03
A71	3.18	L134	3.01
V72	4.21	L152	2.93
E73	3.79	D153	2.01
R74	3.31	K154	1.92
Y75	3.11	V190	3.72
L76	2.48	L191	2.16
D78	1.27	S192	2.40
Q79	0.27	I193	0.68
Q80	1.25	V194	-0.49
L81	1.61		
L82	1.58		
G83	1.10		
I84	1.85		
W85	1.25		
G86	1.04		

## Extended Model-free Analysis

**Table S2.** Input experimental data for the Extended Model-free analysis and back-calculated data for quality assessment of the fit (this table is related to the Results section “Inter-domain dynamics” and Table 1). Average experimental data and error-weighted standard deviation for clusters of residues with similar dynamic properties in gp41<sup>27-194</sup> that were used as input for the extended model-free analysis are shown (Input). Back-calculated relaxation data are shown (Back-calculated) that were calculated using the model-free parameters shown in Table 1.

Input								
	$R_1$ [s <sup>-1</sup> ]	$R_1$ [s <sup>-1</sup> ]	$R_2$ [s <sup>-1</sup> ]	$R_2$ [s <sup>-1</sup> ]	$I/I_0$	$I/I_0$	$\eta_{xy}$ [s <sup>-1</sup> ]	$\eta_{xy}$ [s <sup>-1</sup> ]
Cluster	600 MHz	800 MHz	600 MHz	800 MHz	600 MHz	800 MHz	600 MHz	800 MHz
55-78	0.81 ±0.04	0.61 ±0.03	39.1 ±2.8	49.0 ±3.8	0.63 ±0.06	0.71 ±0.05	27.7 ±3.1	35.7 ±2.8
83-102	1.12 ±0.04	0.95 ±0.04	20.2 ±3.0	24.2 ±3.6	0.39 ±0.07	0.50 ±0.06	13.5 ±2.5	17.4 ±2.7
119-133	0.81 ±0.05	0.62 ±0.05	41.8 ±5.3	50.7 ±5.3	0.59 ±0.06	0.67 ±0.05	30.1 ±5.1	32.4 ±3.4
190-194	0.81 ±0.13	0.66 ±0.09	44.6 ±4.6	47.6 ±2.0	0.54 ±0.10	0.56 ±0.11	28.2 ±4.1	40.1 ±3.7
Back-calculated								
55-78	0.80 ±0.03	0.63 ±0.02	38.2 ±1.5	46.9 ±1.8	0.67 ±0.04	0.69 ±0.04	29.0 ±1.1	38.5 ±1.5
83-102	1.11 ±0.03	0.96 ±0.04	19.2 ±1.5	23.4 ±1.9	0.42 ±0.05	0.46 ±0.03	14.5 ±1.2	19.2 ±1.6
119-133	0.80 ±0.04	0.64 ±0.04	37.3 ±1.9	45.7 ±2.3	0.62 ±0.04	0.65 ±0.04	28.3 ±1.4	37.6 ±1.9
190-194	0.75 ±0.07	0.64 ±0.07	39.0 ±1.4	47.9 ±1.7	0.55 ±0.06	0.62 ±0.07	29.6 ±1.1	39.4 ±1.4



## NMR backbone assignment data

**Table S3.** Chemical shift assignments for the studied gp41<sup>27-194</sup> construct in DPC micelles (related to the Experimental Procedures section “NMR spectroscopy” and Figure 1). The table is provided as a separate Excel document.

## <sup>15</sup>N Relaxation data

**Table S4A.** <sup>15</sup>N R<sub>1</sub>, <sup>15</sup>N R<sub>2,0</sub> (derived from <sup>15</sup>N R<sub>1,ρ</sub>), {<sup>1</sup>H}-<sup>15</sup>N NOE, transverse <sup>15</sup>N CSA –dipolar cross-correlated relaxation data η<sub>xy</sub> and <sup>15</sup>N R<sub>2,β</sub> relaxation data for gp41<sup>27-194</sup>, measured at 600 MHz and 800 MHz. This table is related to the Results section “Inter-domain dynamics” and Figure 2) and provided as a separate Excel document.

## Lipid- and solvent PRE measurements

**Table S5.** Lipid (5-DSA) and solvent (Omniscan) PRE data. Intensities are normalized relative to a reference sample of identical gp41 and DPC concentration (related to Figure 3).

	$I/I_0$	$\Delta I/I_0$	$I/I_0$	$\Delta I/I_0$
	5-DSA		Omniscan	
V28	0.46	0.01	0.3	0.01
Q29	0.55	0.01	0.34	0.01
A30	0.56	0.02	0.44	0.01
R31	0.81	0.02	0.58	0.02
Q32	0.86	0.01	0.61	0.01
L33	0.76	0.01	0.66	0.01
L34	0.69	0.01	0.74	0.01
S35	0.76	0.02	0.69	0.02
G36	0.76	0.01	0.58	0.01
I37	0.75	0.02	0.73	0.02
V38	0.76	0.02	0.72	0.02
Q39	0.70	0.02	0.69	0.02
Q40	0.86	0.02	0.6	0.02
N42	0.85	0.02	nd	nd
N43	0.93	0.03	0.51	0.02
L44	0.54	0.02	0.61	0.02
R46	0.87	0.03	0.77	0.03
A47	0.78	0.02	0.73	0.02
I48	0.82	0.02	0.76	0.02
H53	0.76	0.05	nd	nd
L54	0.73	0.02	0.67	0.02
L57	0.85	0.02	nd	nd
T58	0.76	0.05	0.65	0.05
V59	0.74	0.02	0.74	0.02
G61	0.72	0.05	0.67	0.05
I62	0.62	0.02	0.73	0.02
Q64	0.79	0.02	0.58	0.02
L65	0.70	0.02	0.54	0.01
Q66	0.55	0.03	0.7	0.03
A67	0.50	0.01	nd	nd
L70	0.70	0.02	0.67	0.02
A71	0.82	0.03	0.7	0.03
E73	0.57	0.02	0.55	0.02
R74	0.90	0.02	0.48	0.01
Y75	0.73	0.03	0.5	0.02
L76	0.87	0.02	0.77	0.02

D78	0.70	0.02	0.52	0.02
L81	0.76	0.01	0.6	0.01
L82	0.67	0.02	0.62	0.02
G83	0.44	0.02	0.54	0.02
I84	0.68	0.02	0.67	0.02
W85	0.64	0.02	0.64	0.02
G86	0.48	0.02	0.52	0.02
A87	0.66	0.01	0.5	0.01
S88	0.73	0.01	0.46	0.01
G89	0.74	0.02	0.47	0.01
K90	0.82	0.01	0.55	0.01
L91	0.62	0.01	0.7	0.01
I92	0.75	0.01	0.66	0.01
T95	0.66	0.02	0.55	0.02
A96	0.54	0.01	0.54	0.01
V97	0.59	0.02	0.58	0.02
N100	0.44	0.03	0.53	0.03
A101	0.62	0.01	0.41	0.01
W103	0.75	0.02	nd	nd
S104	0.66	0.01	0.43	0.01
N105	0.66	0.03	nd	nd
S107	0.73	0.02	0.44	0.01
L108	0.47	0.03	0.52	0.03
Q109	0.74	0.03	0.55	0.02
Q110	0.82	0.02	0.5	0.02
D121	0.69	0.04	0.51	0.04
I124	0.69	0.03	0.64	0.03
N125	0.78	0.02	0.53	0.02
N126	0.88	0.01	0.45	0.01
T128	0.81	0.05	nd	nd
S129	nd	nd	0.51	0.02
L130	0.87	0.02	0.59	0.02
I131	0.81	0.01	0.66	0.01
H132	0.75	0.02	0.7	0.02
S133	0.85	0.03	0.59	0.02
L134	0.49	0.02	0.41	0.02
D153	0.84	0.03	0.56	0.03
V190	0.66	0.04	0.77	0.04
L191	0.78	0.01	0.61	0.01
S192	0.59	0.04	0.51	0.03
I193	0.71	0.04	0.61	0.04
V194	0.58	0.04	0.37	0.04

## **Supplemental References**

Lakomek, N.A., Kaufman, J.D., Stahl, S.J., Louis, J.M., Grishaev, A., Wingfield, P.T., and Bax, A. (2013). Internal Dynamics of the Homotrimeric HIV-1 Viral Coat Protein gp41 on Multiple Time Scales. *Angew Chem Int Edit* 52, 3911-3915.